Hyperfine Anomaly Measurements in Francium Isotopes and the Radial Distribution of Neutrons

J. S. Grossman, L. A. Orozco, M. R. Pearson, J. E. Simsarian,* G. D. Sprouse, and W. Z. Zhao†
Department of Physics and Astronomy, State University of New York, Stony Brook, New York 11794-3800
(Received 5 April 1999)

We have measured the hyperfine structure of the $7P_{1/2}$ level for $^{208-212}$Fr to a precision of 300 ppm. These measurements along with previous ground state hyperfine structure measurements reveal a hyperfine anomaly. The hyperfine anomaly exhibits a strong sensitivity to the radial distribution of the neutron magnetization, providing a good way to probe this quantity. We use neutron radial distributions from recent theories to qualitatively explain the measurements.

PACS numbers: 21.10.Gv, 27.80.+w, 32.10.Fn

One of the properties of nuclei that can be probed with precise measurements of hyperfine structure is the nuclear magnetization distribution. The Bohr-Weisskopf effect [1,2] has been known for many years, but experimental and theoretical advances have now allowed more broadly based and detailed investigations [3–6]. There is much interest in obtaining the structural details of heavy nuclei, as these nuclei are involved in understanding quantum electrodynamic (QED) effects in heavy atoms [7], atomic parity nonconservation (PNC), time reversal violation, and nuclear anapole moments [8]. We have measured five different Fr isotopes. Comparison of adjacent isotopes allows extraction of the nuclear magnetization distribution of the last neutron, a quantity that is, in general, very difficult to study [9].

Bohr-Weisskopf effect measurements usually require detailed knowledge of both hyperfine structure constants and magnetic moments. We show in this Letter that precision measurements of the hyperfine structure in atomic states with different radial distributions can give information on the hyperfine anomaly [10] and be sensitive to the nuclear magnetization distribution. Laser trapped radioactive atoms, cooled to μK temperatures, are an ideal sample for high precision Doppler-free laser spectroscopy [8]. High precision allows searching for higher order effects in the hyperfine structure.

Francium is an excellent element for understanding the atom-nucleus hyperfine interactions, and eventually weak interactions. First, because of the large Z, hyperfine effects proportional to Z^3 are larger than in lighter atoms. Second, the simple atomic structure allows *ab initio* calculations of its properties [11–13] that have been experimentally tested [14]. Third, Fr has a large number of isotopes spanning almost 30 neutrons with lifetimes greater than 1 s that cover a wide range of nuclear structure. Fourth, because of its proximity to Pb, where the charge radii are known extremely well from many techniques [15], we can determine the charge radii of the light Fr isotopes with some confidence.

Coc *et al.* [16,17] measured the $7S_{1/2}$ ground state hyperfine constants for 16 Fr isotopes, but only one magnetic moment has been measured [18]. We have focused on extracting hyperfine anomaly information using the available data in the literature and our new precision spectroscopy of the $7P_{1/2}$ hyperfine structure on five francium isotopes. Previous measurements of the $7P_{1/2}$ [17] were not of sufficient precision to observe the small hyperfine anomaly effects. The recent measurement of ^{221}Fr [19] has better precision but still not sufficient to adequately delineate small effects. The $7P_{1/2}$ electron probes the nucleus with a more uniform radial dependence of the interaction than does the $7S_{1/2}$ electron. The ratio of the hyperfine constants is sensitive to the nuclear magnetization distribution. Since both states are spin-$\frac{1}{2}$, the measurements are independent of quadrupole effects that complicate the extraction of precise magnetic hyperfine structure constants.

The magnetic hyperfine interaction can be written as [2]

$$W^l_{\text{extended}} = W^l_{\text{point}}[1 + \epsilon(A, l)], \tag{1}$$

where ϵ is a small quantity that depends on the particular isotope, A, and an atomic state, $l = S$ or P. The ratio, ρ, of hyperfine structure constants in the S and P states is given by

$$\begin{aligned} \rho_A &= \frac{W^S_{\text{extended}}}{W^P_{\text{extended}}} = \frac{W^S_{\text{point}}[1 + \epsilon(A, S)]}{W^P_{\text{point}}[1 + \epsilon(A, P)]}, \\ \rho_A &\approx \rho_0[1 + \epsilon(A, S) - \epsilon(A, P)], \end{aligned} \tag{2}$$

where ρ_0 is the ratio of hyperfine structure constants for a point nucleus. Here, we have neglected the weak dependence of the hyperfine constants on the finite size of the charge distribution (Breit-Rosenthal effect). This correction to ρ was calculated for the $7S_{1/2}$ and $6P_{1/2}$ states in nearby Tl nuclei as 11.7×10^{-4} fm^{-2} [3]. For the Fr isotopes that we are considering, the fractional change in ρ between adjacent isotopes from this effect is less than 10^{-4}. Equation (2) shows that the ratio ρ_A can have a different value for different isotopes because the S and P states have different sensitivity to the nuclear magnetization distribution. Since the error in the measurement comes from two hyperfine splittings, it is very important to have as accurate as possible numbers for especially the excited state splitting.

 © 1999 The American Physical Society

We capture a sample of the radioactive Fr isotope of interest in a magneto-optical trap (MOT) on line at the Stony Brook LINAC. We then measure the hyperfine splitting in the excited $7P_{1/2}$ state in this Doppler-free sample. Heavy ion fusion reactions create $^{208-212}$Fr isotopes with the reactions ^{16,18}O(^{197}Au, xn)$^{208-211}$Fr, and ^{19}F(^{198}Pt, $5n$)^{212}Fr. We obtain typically 10^6 Fr/s and transport them into the MOT as described previously [14]. Three Ti:sapphire lasers excite different atomic transitions as shown in Fig. 1. Two lasers form the MOT: a trap laser on the D_2 cycling transition and a repump laser on the D_1 transiton to return atoms from the low F ground state to the trapping cycle [8]. We excite the hyperfine splitting of the $7P_{1/2}$ state with a 40 ns pulse from a third probe laser. We detect for 60 ns the fluorescence decay with an f/1.5 optical system and a Hamamatsu R636 photomultiplier while the repump laser is off for 0.3 μs during each cycle of 10 μs. See Fig. 1 for the timing sequence. A computer controlled Fabry-Pérot cavity stabilizes and monitors the long term frequency of all of the lasers [20].

The measurement technique transfers the hyperfine splitting into a frequency measurement. We frequency modulate (FM) the probe laser with an electro-optic modulator. The resulting beam has FM sidebands at approximately ± 3 GHz off the carrier as shown in Fig. 1. The sidebands excite the two hyperfine components of the $7P_{1/2}$ hyperfine splitting as we scan the carrier. The sidebands span most of the splitting and the carrier only has to scan a small frequency interval to reach the two lines. See Fig. 2 for an example of the data. We repeat the scans with different rf frequencies choosing values to have the sidebands larger or smaller than the hyperfine splitting. We find the splitting by interpolating to zero on a least squares fit of the line positions versus the modulation frequency. For ^{208}Fr and ^{212}Fr, the errors are larger because the zero crossing frequency was extrapolated from the fits. The accuracy is set by the stability of the microwave generator, the signal-to-noise ratio of the resonance, and the linearity of the scan. The resonant repump laser was on at the same time as the probe laser in order to maximize the excited state population. This transition is not cycling, and with the intensity we had (2 mW/cm^2) we could not observe any shift or broadening; an equivalent Rabi frequency for this intensity in the case of a two level atom would correspond to less than 2 MHz. The lambda transition to the other hyperfine ground state was also greatly suppressed by the low power in the probe laser. We did not find any systematic dependence of the resonance positions with trap laser power, trap laser detuning, or probe laser power. Auxiliary experiments with Rb allowed us to place an upper limit on a Zeeman shift of 0.8 MHz. Table I shows the hyperfine intervals of the $7P_{1/2}$ state for the five isotopes from this work along with the ground state hyperfine intervals determined in Ref. [16]. The errors in our measurement include the statistical uncertainties from the fits and the systematic contributions stated above. Figure 3 shows the ratios of the $7S_{1/2}$ to $7P_{1/2}$ hyperfine A constants for different isotopes. We observe a distinctive odd-even alternation well beyond the size

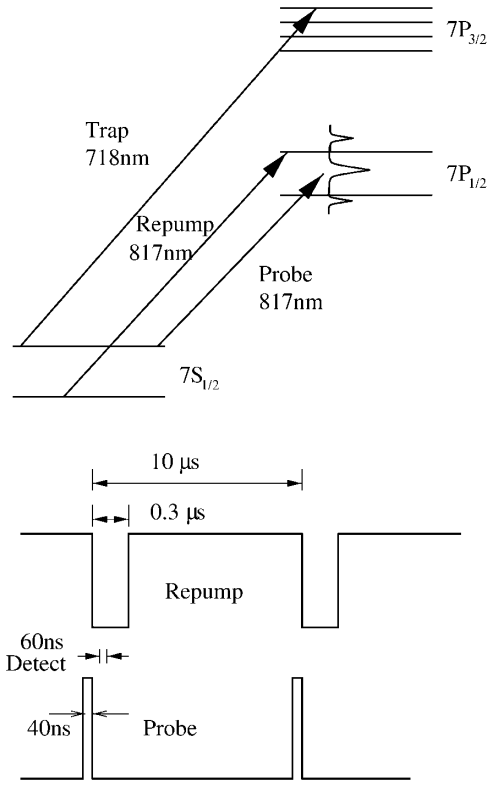

FIG. 1. Energy levels and time sequence for excitation and detection. The sidebands on the probe laser are indicated schematically.

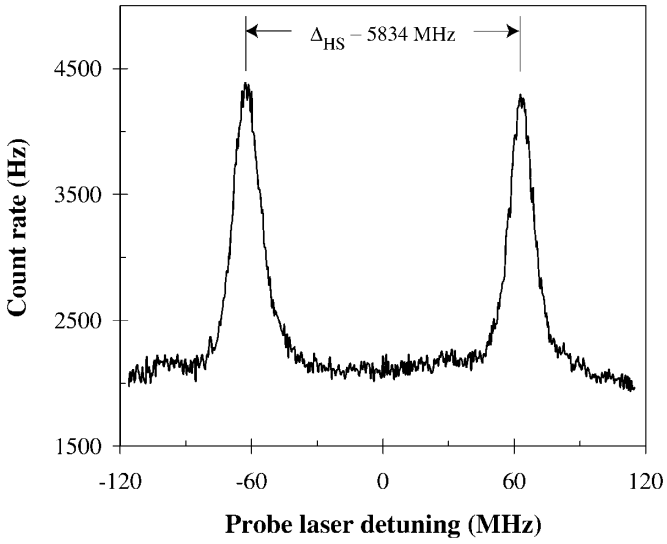

FIG. 2. Scan of the $7P_{1/2}$, $F = 4$ and $F = 5$ hyperfine states of ^{211}Fr. The peak separation is the hyperfine splitting minus twice the modulation frequency.

TABLE I. Hyperfine A coefficients for $^{208-212}$Fr.

Isotope	$A(7p_{1/2})$	$A(7s_{1/2})$	$A(7s)/A(7p)$
208	874.8(3)	6650.7(8)	7.6024(23)
209	1127.9(2)	8606.7(9)	7.6306(15)
210	946.3(2)	7195.1(4)	7.6043(11)
211	1142.1(2)	8713.9(8)	7.6300(19)
212	1192.0(2)	9064.2(2)	7.6048(18)

of our error bars. The three lines on the graph result from our calculations of the hyperfine anomaly and will be discussed below.

A calculation of ϵ must be carried out which has accurate knowledge of both the atomic and the nuclear structure in order to fully understand the observations and learn as much as we can about the distribution of neutrons in nuclei. For the atom, the Dirac equation must be solved and the many body correlations of the atomic core included. For the nucleus, the nuclear magnetization distribution must be calculated from a nuclear model. The additional experimental information provided by the hyperfine anomaly and the charge radii can help to further constrain the model to give correct radial distributions of both neutrons and protons. We hope that these new results will motivate such a calculation.

Here, we will use available models to see if we can explain qualitatively the observed changes in ρ. We estimate the charge radii of the Fr isotopes by observing that the isotope shifts of the light Fr nuclei are linearly proportional to the Pb charge radii for the same neutron number [21]. The absolute rms charge radii of many of the Pb isotopes have been determined to a precision of 7×10^{-4} fm by combining optical, x-ray, mu-mesic, and

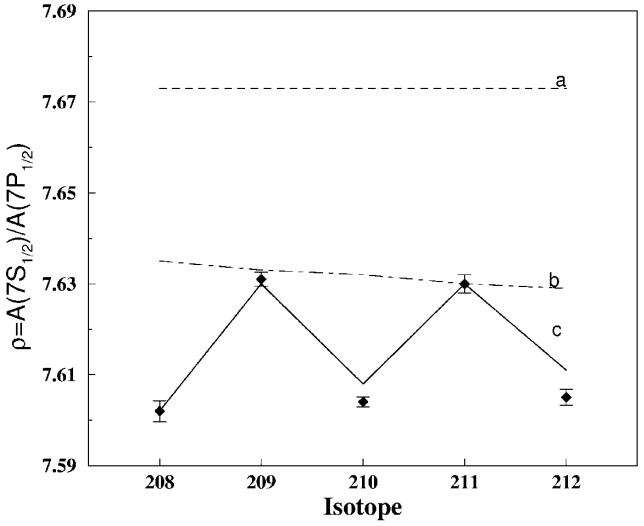

FIG. 3. Ratio of hyperfine A magnetic dipole constants of $7S_{1/2}$ and $7P_{1/2}$ states and differential changes observed for five different Fr isotopes. *a*: point nucleus; *b*: charge radius equal to magnetic radius; *c*: Stroke calculation method.

electron scattering data [15]. We extract the $\delta\langle r^2\rangle_c$ of Fr from the isotope shifts [17], and we take the isotonic dependence from Brown [22]. From this we arrive at the rms charge radii given in Table II.

Dzuba *et al.* [11] have studied the effect of the finite nuclear magnetization on the hyperfine structure constants in francium. The ratio of hyperfine interaction constants calculated for several different values of the rms radius of the magnetization in the range $\langle r^2\rangle_m^{1/2}$ between 4–6.5 fm can be parametrized as

$$\rho = \rho_0(1 - \lambda_m\langle r^2\rangle_m^{1/2}), \tag{3}$$

where $\lambda_m = +0.0046$ fm^{-1}. These test calculations did not include correlations. We will assume that the correlations have the same radial dependence as the main terms in order to estimate the changes in $\langle r^2\rangle_m^{1/2}$ that cause the observed changes in the ratio of hyperfine constants.

Let us first assume that the magnetization radius $\langle r^2\rangle_m^{1/2}$ is the same as the charge radius $\langle r^2\rangle_c^{1/2}$. With this assumption, the dependence of the hyperfine constant ratio on the radial distribution of magnetization is shown in trace *b* of Fig. 3. This assumption is consistent with the observations of the two even N nuclei, ^{209}Fr and ^{211}Fr, but not with the large deviations seen for nuclei with an odd number of neutrons. We see that the changes in the magnetization radii for the odd neutron nuclei are much larger than the changes that can be associated with just the charge radii alone.

The magnetic moments of the Fr isotopes can be estimated by using the known moment of ^{211}Fr [18] and the ratios of the hyperfine structure constants (neglecting the small hyperfine anomaly). The shell model then successfully explains the trends of the magnetic moments of the light Fr isotopes near $N = 126$ [18]. Table II shows the moments and configurations of these nuclei. We have calculated the Bohr-Weisskopf effect, ϵ, for each of these states with the procedures and formulas in Ref. [2]. The nuclear radial matrix elements for the $\pi h_{9/2}$, $\nu f_{5/2}$, and $\nu p_{1/2}$ orbitals were obtained from spherical Hartree-Fock calculations and a new Skyrme interaction [22]. We use effective g factors which describe the observed magnetic moments (see Table II) and obtain ϵ (in %) for the $\pi h_{9/2}$, $\nu f_{5/2}$, and $\nu p_{1/2}$ orbitals of -0.56, -1.97, and -2.44, respectively. The ϵ for odd-odd nuclei were calculated using the relation in [5]. The values obtained are in good agreement with our measurements (see trace *c* in Fig. 3). The variation with isotope of the ratio of hyperfine constants exhibits only the differences between the even and odd N cases. We can estimate the ratio for point nuclei as $\rho_0 = 7.673$ by taking the theoretical value and the average experimental ratio for the two even-N isotopes ^{209,211}Fr (see trace *a* in Fig. 3).

Although the nuclear moment of Fr isotopes is generated primarily by the last unpaired $h_{9/2}$ proton, we see that the effect of the larger radial distribution of the neutrons gives rise to measurable effects in the hyperfine constant

TABLE II. Parameters used in the calculation of the Bohr-Weisskopf effect.

A	208	209	210	211	212
Configuration	$\pi h_{9/2} \otimes \nu f_{5/2}$	$\pi h_{9/2}$	$\pi h_{9/2} \otimes \nu f_{5/2}$	$\pi h_{9/2}$	$\pi h_{9/2} \otimes \nu p_{1/2}$
Spin	7	9/2	6	9/2	5
$r_{\rm rms}$ (fm)	5.551	5.558	5.560	5.566	5.570
$\epsilon(\%)$ (theory)	−0.92	−0.56	−0.84	−0.56	−0.80
μ (experimental) (μ_N)	4.75(2)	3.95(2)	4.40(9)	4.00(9)	4.62(9)
$\mu(g_{l\pi} = 1.16, g_{l\nu} = 0, g_{s\pi,\nu} = 0.85 g_s(\text{free}))$	4.91	3.75	4.32	3.75	4.29

ratio. Qualitatively, we see that this sensitivity to the neutron magnetization distribution is explained well by the calculations, except for ^{212}Fr, where the spin of 5 allows mixing of both $\nu f_{5/2}$ and $\nu p_{1/2}$ orbitals into the wave function.

We have measured the hyperfine splitting of the $7P_{1/2}$ excited state in five Fr isotopes with a precision of 300 ppm. The results are sensitive to the radial distribution of the nuclear magnetization, and can be qualitatively understood within a simple picture where the effect is attributed to the unpaired nucleons, as identified by the shell model. These measurements provide one of the few handles on the neutron radial distribution in nuclei, and will help to constrain nuclear structure calculations. In addition, as the nuclear charge and magnetization radii are better understood, they will help to further test and refine the *ab initio* atomic calculations which are of crucial importance to the understanding of PNC and QED effects in atoms. The light francium isotopes form a unique laboratory in which detailed calculations of both the nucleus and the atom are possible. More refined calculations in both systems should be able to eliminate many of the uncertainties which have clouded our understanding of the electron-nucleus interactions.

This work is supported in part by NSF and NIST.

*Present address: NIST, Gaithersburg, Maryland 20899-8424.

†Present address: Sensitron Semiconductor, Deer Park, New York 11729.

[1] A. Bohr and V. F. Weisskopf, Phys. Rev. **77**, 94 (1950).

[2] H. H. Stroke, R. J. Blin-Stoyle, and V. Jaccarino, Phys. Rev. **123**, 1326 (1961).

[3] A.-M. Mårtensson-Pendrill, Phys. Rev. Lett. **74**, 2184 (1995).

[4] T. Kühl, A. Dax, M. Gerlach, D. Marx, H. Winter, M. Tomaselli, T. Engel, M. Würtz, V. M. Shabaev, P. Seelig, R. Grieser, G. Huber, P. Merz, B. Fricke, and C. Holbrow, Nucl. Phys. **A626**, 235 (1997).

[5] S. Büttgenbach, Hyperfine Interact. **20**, 1 (1984).

[6] J. R. Crespo López-Urrutia, P. Beiersdorfer, K. Widmann, B. B. Birkett, A.-M. Mårtensson-Pendrill, and M. G. H. Gustavsson, Phys. Rev. A **57**, 879 (1998).

[7] M. Tomaselli, T. Kühl, P. Seelig, C. Holbrow, and E. Kankeleit, Phys. Rev. C **58**, 1524 (1998).

[8] G. D. Sprouse and L. A. Orozco, Annu. Rev. Nucl. Part. Sci. **47**, 429 (1997).

[9] H. T. Duong, C. Ekström, M. Gustafsson, T. T. Inamura, P. Juncar, P. Lievens, I. Lindgren, S. Matsuki, T. Murayama, R. Neugart, T. Nilsson, T. Nomura, M. Pellarin, S. Penselin, J. Persson, J. Pinard, I. Ragnarsson, O. Redi, H. H. Stoke, J. L. Vialle, and the ISOLDE Collaboration, Nucl. Instrum. Methods Phys. Res., Sect. A **325**, 465 (1993).

[10] J. R. Persson, Eur. Phys. J. A **2**, 3 (1998).

[11] V. A. Dzuba, V. V. Flambaum, and O. P. Sushkov, J. Phys. B **17**, 1953 (1984).

[12] V. A. Dzuba, V. V. Flambaum, and O. P. Sushkov, Phys. Rev. A **51**, 3454 (1995).

[13] W. R. Johnson, Z. W. Liu, and J. Sapirstein, At. Data Nucl. Data Tables **64**, 279 (1996).

[14] See, for example, J. E. Simsarian, L. A. Orozco, G. D. Sprouse, and W. Z. Zhao, Phys. Rev. A **57**, 2448 (1998).

[15] G. Fricke, C. Bernhardt, K. Heilig, L. A. Schaller, L. Schellenberg, E. B. Shera, and C. W. de Jager, At. Data Nucl. Data Tables **60**, 177 (1995).

[16] A. Coc, C. Thibault, F. Touchard, H. T. Duong, P. Juncar, S. Liberman, J. Pinard, J. Lermé, J. L. Vialle, S. Büttgenbach, A. C. Mueller, A. Pesnelle, and the ISOLDE Collaboration, Phys. Lett. **163B**, 66 (1985).

[17] A. Coc, C. Thibault, F. Touchard, H. T. Duong, P. Juncar, S. Liberman, J. Pinard, M. Carre, J. Lermé, J. L. Vialle, S. Büttgenbach, A. C. Mueller, A. Pesnelle, and the ISOLDE Collaboration, Nucl. Phys. **A468**, 1 (1987).

[18] C. Ekström, L. Robertsson, and A. Rosén, Phys. Scr. **34**, 624 (1986).

[19] Z.-T. Lu, K. L. Corwin, K. R. Vogel, C. E. Wieman, T. P. Dinneen, J. Maddi, and Harvey Gould, Phys. Rev. Lett. **79**, 994 (1997).

[20] W. Z. Zhao, J. E. Simsarian, L. A. Orozco, and G. D. Sprouse, Rev. Sci. Instrum. **69**, 3737 (1998).

[21] J. Billowes and P. Campbell, J. Phys. G **21**, 707 (1995).

[22] B. A. Brown, Phys. Rev. C **58**, 220 (1998); (private communication).